Remote Sensing Image Enhancement Using Regularized-Histogram Equalization and DCT

Xueyang Fu, Jiye Wang, Delu Zeng, Yue Huang, and Xinghao Ding, *Member, IEEE*

***Abstract*—In this letter, an effective enhancement method for remote sensing images is introduced to improve the global contrast and the local details. The proposed method constitutes an empirical approach by using the regularized-histogram equalization (HE) and the discrete cosine transform (DCT) to improve the image quality. First, a new global contrast enhancement method by regularizing the input histogram is introduced. More specifically, this technique uses the sigmoid function and the histogram to generate a distribution function for the input image. The distribution function is then used to produce a new image with improved global contrast by adopting the standard lookup table-based HE technique. Second, the DCT coefficients of the previous contrast improved image are automatically adjusted to further enhance the local details of the image. Compared with conventional methods, the proposed method can generate enhanced remote sensing images with higher contrast and richer details without introducing saturation artifacts.**

***Index Terms*—Contrast enhancement, discrete cosine transform (DCT), histogram, image enhancement, remote sensing images.**

I. Introduction

THE demand of high-quality remote sensing images is rapidly increasing due to the wide spread use of these images in various applications such as military, geosciences, agriculture, and astronomy. The undesirable environmental conditions reduce the contrast and the hidden details of the captured remote sensing images. Since contrast is an important quality factor in remote sensing images [1], therefore, contrast enhancement techniques are required for better information representation and visual perception.

In general, the contrast enhancement methods can be divided into two categories, i.e., image spatial-domain methods and transform-domain methods. Among the image spatial-domain algorithms, the traditional histogram equalization (HE) [2] is the most widely used algorithm due to its simple and effective implementation. However, the main disadvantage of HE is that the generated result is overenhanced if there are peaks in the histogram. This leads to a saturation artifact and harsh appearance in the enhanced resultant image. To overcome this problem, some histogram-based methods in the image spatial domain have been proposed, e.g., brightness-preserving dynamic HE [3] and histogram modification framework [4]. Although the two methods can effectively avoid overenhancement, the details are not prominently emphasized due to the fact that both of these methods primarily preserve the shape of the input histogram. Recently, another contrast enhancement method has been proposed that uses an adaptive gamma correction with weighting distribution (AGCWD) [5]. This method can produce comparable results, but it may also result in saturation artifacts and loss of details in bright regions. The 2-D histogram-based methods, which use contextual information to enhance the contrast of the input image, are proposed in [6]–[8]. However, creating a 2-D histogram is computationally expensive, which is not suitable for many practical applications.

Transform-domain methods decompose an input image into different subbands and enhance the contrast by modifying specific components [6]. In [9], a singular value equalization method is proposed to adjust the image brightness. This method is further improved by combining with discrete wavelet transform in [1] to achieve better contrast enhancement results. Another method, which uses discrete wavelet transform and adaptive intensity transformation to enhance the contrast of remote sensing images, is proposed in [10]. This method requires appropriate settings of the associated parameters, which makes it unfit for practical use. A subband-decomposed multiscale retinex method combined with a hybrid intensity transfer function is introduced in [11] to enhance the optical remote sensing images. In [12], a general illumination normalization method for multiple remote sensing images is proposed. This method first enhances the contrast in the gradient domain and then equalizes the singular value to adjust the brightness. However, contrast and details are not obviously emphasized since this algorithm primarily maintains the illumination consistency.

In this letter, a novel and empirical enhancement method for remote sensing images is proposed to improve the global contrast and emphasize the local details. First, a new global contrast enhancement algorithm without the need of any parameter selection is presented. This new algorithm can be considered as an improvement of the traditional HE method. More specifically, the algorithm generates a new distribution function to regularize the input histogram by using the sigmoid function. The algorithm further maps the newly generated distribution function to a uniform distribution function. This uniform distribution

Manuscript received May 30, 2015; revised July 7, 2015 and August 19, 2015; accepted August 24, 2015. Date of publication September 18, 2015; date of current version October 27, 2015. This work was supported in part by the National Natural Science Foundation of China under Grants 61103121, 81301278, 61571382, and 61571005, by the Fundamental Research Funds for the Central Universities under Grants 20720150169 and 2072015009, and by the Research Fund for the Doctoral Program of Higher Education under Grant 20120121120043. *(Corresponding author: Xinghao Ding.)*

X. Fu, D. Zeng, Y. Huang, and X. Ding are with the Fujian Key Laboratory of Sensing and Computing for Smart Cities, School of Information Science and Engineering, Xiamen University, Xiamen 361006, China (e-mail: dxh@xmu.edu.cn).

J. Wang is with State Grid Corporation of China, Beijing 100031, China.

Color versions of one or more of the figures in this letter are available online at http://ieeexplore.ieee.org.

Digital Object Identifier 10.1109/LGRS.2015.2473164

function is used to obtain the global contrast enhanced image by adopting a standard lookup table-based HE procedure. Second, the discrete cosine transform (DCT) coefficients of the previous global contrast enhanced image are empirically adjusted with only one parameter to further emphasize on the local details. Moreover, a simple but effective thresholding approach is also presented with an automatic parameter setting design. The final output image is obtained by applying the inverse DCT. Since the advantages of both image spatial-domain (histogram) and transform-domain (DCT) methods are involved in the proposed method, the enhanced remote sensing image is characterized by high global contrast and rich local details. Meanwhile, the proposed method does not introduce unpleasing saturation artifacts like other contrast enhancement methods. Experimental results have demonstrated that the proposed method can generate promising results in both qualitative and quantitative assessments.

II. Proposed Algorithm

A. Global Contrast Enhancement

Suppose an input remote sensing image $\mathbf{X}$ of size $M \times N$ with a dynamic range of $[x_{\min}, x_{\max}]$, where $x_{\min}$ and $x_{\max}$ are the minimum and maximum elements of $\mathbf{X}$, respectively. The goal is to produce an output global contrast enhanced image $\mathbf{Y}_{\text{global}}$ with a new dynamic range of $[y_{\min}, y_{\max}]$. For example, $y_{\min} = 0$ and $y_{\max} = 2^8 - 1 = 255$ for 8-bit images.

Since the traditional HE generates overenhanced results when there exist high peaks in the input histogram, the targeted distribution function for creating the output should be adjusted to avoid this problem. The overenhancement and saturation artifact problem can be effectively avoided by utilizing the smoothness and compression characteristics of the sigmoid function in finely regularizing the input histogram. Thus, a new distribution function f is generated as

$$f(k) = s(k)\,(1 + h(k)) \tag{1}$$

where h is the normalized input histogram; $k = 1, \ldots, K$; and K is the number of the gray levels in the input image $\mathbf{X}$. Sigmoid function s is modified as

$$s(k) = \frac{1}{1 + e^{-(k-1)}} - \frac{1}{2}. \tag{2}$$

This modification assures the minimum of the enhanced image be equal to 0. Distribution function f is further normalized according to

$$f(k) \leftarrow f(k) / \sum_{t=1}^{K} f(t) \tag{3}$$

and uniform distribution function F is computed by

$$F(k) = \sum_{t=1}^{k} f(t). \tag{4}$$

The new gray levels $y(k)$ are computed by using $F(k)$, $y_{\min}$, and $y_{\max}$

$$y(k) = \lfloor F(k)(y_{\max} - y_{\min}) + y_{\min} \rfloor \tag{5}$$

where $\lfloor \cdot \rfloor$ rounds the element to the lower nearest integer. Finally, the global contrast enhanced image $\mathbf{Y}_{\text{global}}$ is obtained by adopting a standard lookup table-based HE procedure with new gray levels.

B. Local Detail Enhancement

In order to enhance both the global contrast and the local details in the remote sensing images, the DCT coefficients of the previous global enhanced image are further adjusted. For the 2-D image, 2-D DCT [2] is adopted to obtain the coefficients. The 2-D DCT coefficients D of size $M \times N$ are computed by

$$D(h,w) = c_h c_w \sum_{i=0}^{M-1} \sum_{j=0}^{N-1} \mathbf{Y}_{\text{global}}(i,j) \cos\left(\frac{\pi(2i+1)h}{2M}\right) \times \cos\left(\frac{\pi(2j+1)w}{2N}\right) \tag{6}$$

where $0 \le i,\ h \le M-1$, $0 \le j,$ and $w \le N-1$. c_h and c_w are computed by

$$c_h = \begin{cases} \sqrt{\frac{1}{M}}, & h = 0 \\ \sqrt{\frac{2}{M}}, & 1 \le h \le M-1 \end{cases} \qquad c_w = \begin{cases} \sqrt{\frac{1}{N}}, & w = 0 \\ \sqrt{\frac{2}{N}}, & 1 \le w \le N-1. \end{cases} \tag{7}$$

Note that lower absolute values of D represent the lower energy components, i.e., details and textures, and vice versa. Moreover, $D(0,0)$ is the largest energy component that represents the mean value of the image. To emphasize the local details, low energy parts should be adjusted, whereas high energy parts should be maintained to avoid any significant change. Based on this analysis, a thresholding algorithm is designed to properly adjust coefficients D by

$$D'(h,w) = \begin{cases} D(h,w), & \text{if } |D(h,w)| > 0.01 \times D(0,0) \\ \alpha D(h,w), & \text{otherwise} \end{cases} \tag{8}$$

where $\alpha > 1$ is the parameter that controls the level of local detail enhancement. Based on the observation of our enhanced results of over 100 images, 0.01 is an appropriate empirical value to separate high and low energy parts. However, a large value of α may result in overenhancement. Thus, a simple automatic parameter setting for α is introduced as

$$\alpha = 1 + \sqrt{\frac{\text{std}(\mathbf{Y}_{\text{global}}) - \text{std}(\mathbf{X})}{2^B - 1}} \tag{9}$$

where B is the image bit depth, and $\text{std}(\mathbf{Y}_{\text{global}})$ and $\text{std}(\mathbf{X})$ are the standard deviations of the previously enhanced image $\mathbf{Y}_{\text{global}}$ and the input image $\mathbf{X}$, respectively. The larger the difference between $\text{std}(\mathbf{Y}_{\text{global}})$ and $\text{std}(\mathbf{X})$ is, the higher local details enhancement is achieved. Lastly, the final enhanced output image $\mathbf{Y}_{\text{final}}$ is obtained by using the inverse 2-D DCT transform [2] of D'.

Fig. 1 shows the enhanced images with different α values. In Fig. 1(b), the local detail enhancement parameter $\alpha = 1$, and

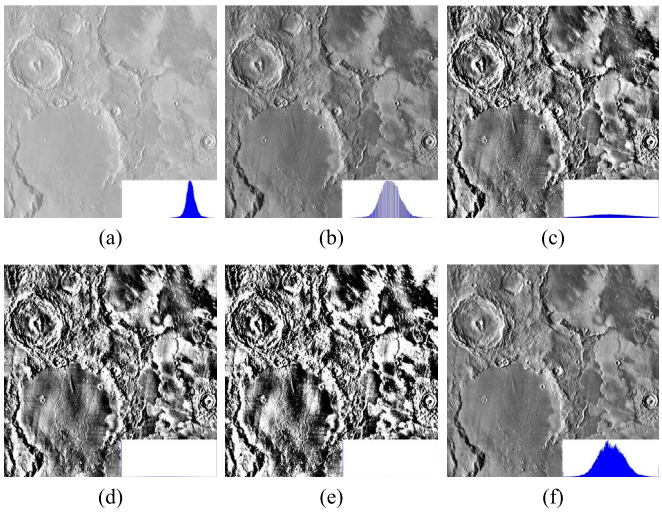

Fig. 1. Results with different α values. (a) Input image. (b) $\alpha = 1$. (c) $\alpha = 3$. (d) $\alpha = 5$. (e) $\alpha = 7$. (f) automatic α setting.

it is shown that the generated result is visually pleasing with no artifacts. Fig. 1(c)–(e) is further improved by local detail enhancement. As α value increases, the edges and the details are becoming increasingly sharper than those in Fig. 1(b). However, a large value of α leads to a visually unpleasing result, as illustrated in Fig. 1(d) and (e). By using the automatic α setting, a good tradeoff between global contrast and local detail enhancement is achieved. The corresponding histograms show that the entire dynamic range has been fully utilized, which means that Fig. 1(f) can provide richer and clearer details than Fig. 1(b) without introducing artifacts.

III. Experimental Results

In this section, the experimental results are presented and are assessed to demonstrate the performance of the proposed method. All experiments have been performed using MATLAB R2014a on a personal computer with 8.0-GB RAM and Intel Core i5-4460U 3.20-GHz CPU. Due to space limitations, only the results of four test images have been shown in this letter. More results and the MATLAB source code are shared at http://smartdsp.xmu.edu.cn/RemoteEnhancement.html.

A. Qualitative Assessments

The proposed method is compared with the traditional HE [2], one image spatial domain method: AGCWD [5] and one transform domain method based on discrete wavelet transform and singular value decomposition: DWT-SVD [1].

Figs. 2–5 present the comparisons of the different remote sensing images with corresponding histograms. All of the input images have low global contrast, and the local details cannot be observed clearly. The traditional HE method [2] can effectively improve the global contrast. However, overenhancement and unpleasing saturation artifacts have appeared in Figs. 2(b)–5(b). For example, in Fig. 2(g), an obvious saturation artifact is shown and the corresponding gradients are not clear, which means that the local details are not enhanced enough. The same phenomenon is shown in the white regions of the background in Figs. 3(b) and 5(b) and tank's surface in Fig. 4(b). The AGCWD method [5] has created more serious saturation artifacts in Figs. 2(c)–5(c), particularly in white regions. The drawback of both HE and AGCWD is mainly caused from the peak in the input histogram. On the contrary, the results of the DWT-SVD method [1] are slightly underenhanced, as shown in Figs. 2(d)–5(d). This is due to the fact that the DWT-SVD method only concentrates on the low–low subband images and ignores the high-frequency parts. Figs. 2(e)–5(e) are the enhanced results produced by the proposed method. Compared with the other three methods, the proposed method has produced results with high global contrast and rich local details. For example, as shown in Fig. 2(j), the local details are well emphasized and the corresponding gradients are relatively clearer. Moreover, the objects are prominent after the enhancement process, such as the tank in Fig. 4(e). Note that many pixels are further accumulated to the extreme values in the histogram of the enhanced images. The main reason for this phenomenon is that the entire dynamic ranges have been fully utilized and black or white details and textures have been further enhanced by adjusting the DCT coefficients.

B. Quantitative Assessments

Two measurements are being used to quantitatively assess the performance of the different methods, as shown in Tables I and II. For each measurement, the best and the second best results are boldfaced and underlined, respectively. One measurement is the discrete entropy (DE) [13], [14], which is computed by

$$\mathrm{DE}(\mathbf{X}) = -\sum_{k=1}^{K} p(x_k) \log p(x_k) \tag{10}$$

where $p(x_k)$ is the probability of the pixel value x_k, which is calculated from the image histogram. Higher value of DE depicts richer details of an image $\mathbf{X}$. As shown in Table I, the proposed method has the highest DE values for all four test images, which implies that Figs. 2(e)–5(e) are providing more useful information.

The second measurement is the contrast gain (CG) [14], which is defined as $CG = C(\mathbf{Y})/C(\mathbf{X})$, where C are the average values of the local contrast measured by the Michelson contrast [15]

$$C_{\mathrm{Michelson}} = \frac{\mathbf{max} - \mathbf{min}}{\mathbf{max} + \mathbf{min}} \tag{11}$$

where $\mathbf{max}$ and $\mathbf{min}$ are the maximum and minimum pixel values in a 3×3 window, respectively. A higher value of CG means a better contrast enhancement. As shown in Table II, the proposed method has outperformed the other algorithms, except the HE. The reason is that the HE algorithm aims to directly map the input histogram to a uniform distribution. Although the HE has the highest CG value, it may still provide the worst visual quality. The reader can take the *Tank* image shown in Fig. 4(b) as an example. Conversely, the proposed method is providing consistently well-enhanced images with the second best CG values. This demonstrates that quantitative assessments of the proposed method are in accordance with the qualitative assessments.

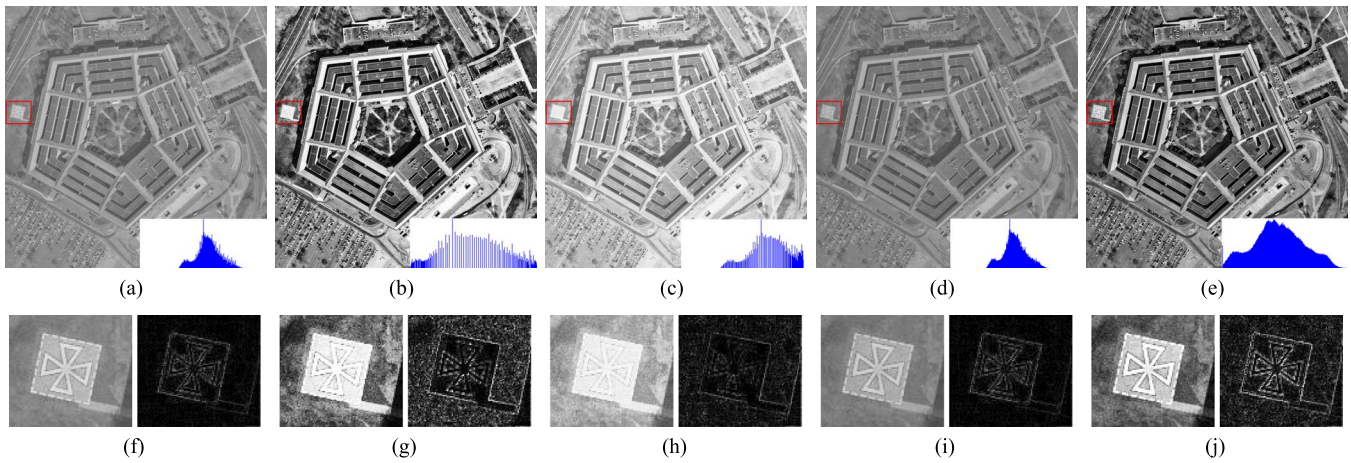

Fig. 2. Comparisons on *The Pentagon* image. (a) Input image. (b) HE. (c) AGCWD. (d) DWT-SVD. (e) Proposed method. (f)–(j) Enlargements and corresponding gradients of (a)–(d) in the red rectangle.

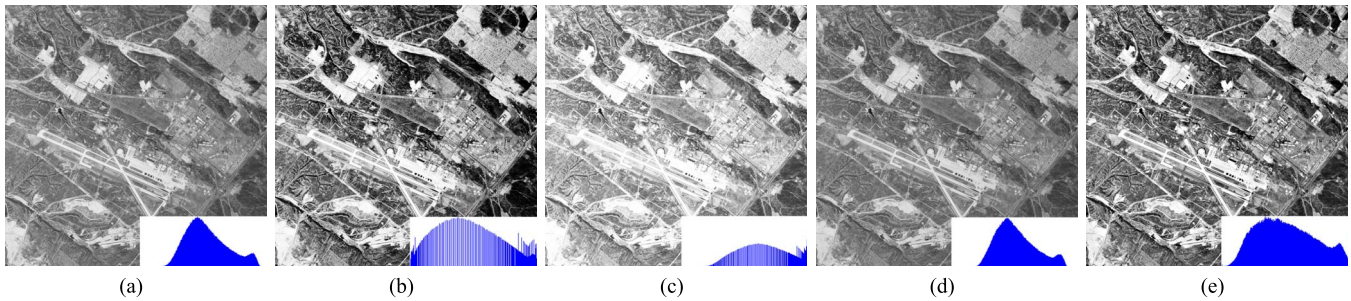

Fig. 3. Comparisons on the *Aerial* image. (a) Input image. (b) HE. (c) AGCWD. (d) DWT-SVD. (e) Proposed method.

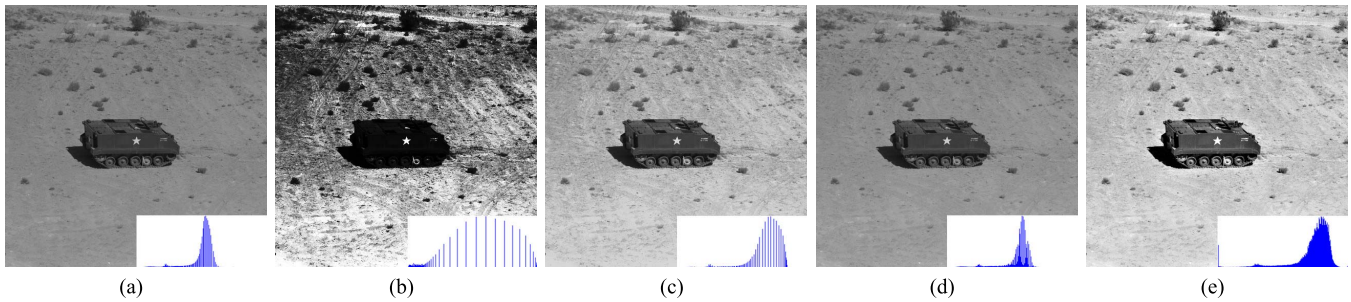

Fig. 4. Comparisons on the *Tank* image. (a) Input image. (b) HE. (c) AGCWD. (d) DWT-SVD. (e) Proposed method.

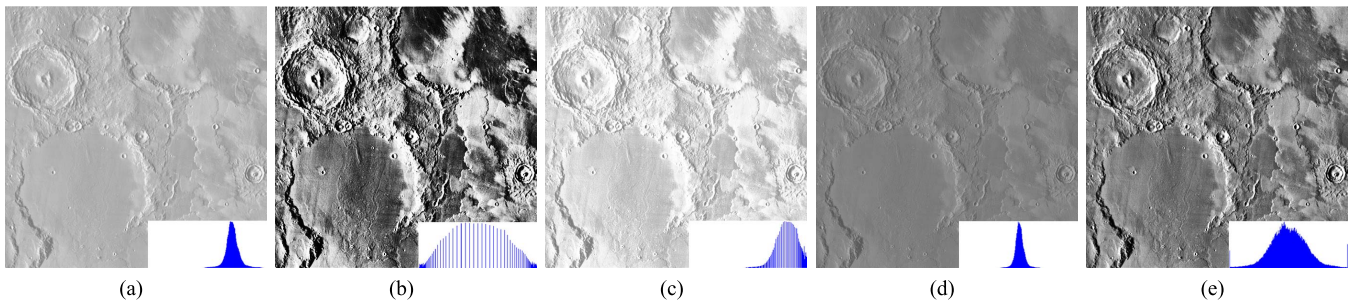

Fig. 5. Comparisons on the *Mars* image. (a) Input image. (b) HE. (c) AGCWD. (d) DWT-SVD. (e) Proposed method.

C. Computation Time

Since the computation time is also an important factor of an algorithm, therefore, the average computation times of four algorithms have been computed and are presented in Table III. A total number of 100 images of size 512 $\times$ 512 have been tested. As shown in Table III, the HE method has the shortest computation time. This is due to the fact that the HE method has the simplest operations to redistribute the image

TABLE I
QUANTITATIVE MEASUREMENT RESULTS OF DE

	Input	HE	AGCWD	DWT-SVD	Proposed
The Pentagon	6.73	6.63	6.54	6.65	**7.76**
Aerial	7.35	7.19	6.97	7.29	**7.83**
Tank	5.05	4.88	5.03	5.62	**6.66**
Mars	5.83	5.69	5.64	5.39	**7.35**

TABLE II
QUANTITATIVE MEASUREMENT RESULTS OF CG

	HE	AGCWD	DWT-SVD	Proposed
The Pentagon	**3.68**	1.30	1.01	3.35
Aerial	**2.49**	1.12	1.02	2.18
Tank	**4.98**	1.49	0.96	1.57
Mars	**8.46**	1.58	1.16	4.75

TABLE III
AVERAGE COMPUTATION TIMES (IN SECONDS)

Image Size	HE	AGCWD	DWT-SVD	Proposed
512×512	0.04	0.17	0.24	0.22

Fig. 6. Ordinary image enhancement. (Left) Input images. (Right) Enhanced results.

histogram. The proposed method has a satisfactory computation time that is comparable to AGCWD and DWT-SVD methods. It is important to highlight that the proposed algorithm has been straightforwardly implemented in MATLAB without optimization. The computational time can be further improved by using C programming and advance computing devices such as graphic processing unit.

D. Extension: Ordinary Image Enhancement

The proposed algorithm is also suitable for ordinary image enhancement. Both gray and color images can be directly processed by our method. For color images, the proposed algorithm is applied to the V component in the HSV color space [2] to preserve the chrominance components. Fig. 6 shows two example images that have been enhanced by the proposed method directly. After our enhancement, the global contrast is well improved in the output images and the objects are more visible and vivid compared with the inputs such as the houses and the car.

IV. CONCLUSION

In this letter, a novel remote sensing image enhancement method has been proposed to improve the image quality. First, a global contrast enhancement technique based on the histogram regularization is introduced. Using sigmoid function combined with the input histogram, a new uniform distribution function is calculated to achieve the global contrast enhancement without requiring any parameter setting. Second, the DCT coefficients of the previously enhanced image are empirically adjusted to further emphasize the local details. The comparison with other enhancement algorithms has proven that the proposed method is capable of generating enhanced remote sensing images not only with high global contrast but also with rich local details without introducing artifacts. Moreover, the proposed method has a satisfactory computation time, which is suitable for enhancement of both remote sensing and ordinary images. In this letter, the proposed method does not consider the noise issue, which would become noticeable after enhancement process. We will further explore this issue in the future work.

REFERENCES

[1] H. Demirel, C. Ozcinar, and G. Anbarjafari, "Satellite image contrast enhancement using discrete wavelet transform and singular value decomposition," *IEEE Geosci. Remote Sens. Lett.*, vol. 7, no. 2, pp. 333–337, Apr. 2010.
[2] R. C. Gonzalez and R. E. Woods, *Digital Image Processing*, 3rd ed. Upper Saddle River, NJ, USA: Prentice-Hall, 2006.
[3] H. Ibrahim and N. S. P. Kong, "Brightness preserving dynamic histogram equalization for image contrast enhancement," *IEEE Trans. Consum. Electron.*, vol. 53, no. 4, pp. 1752–1758, Nov. 2007.
[4] T. Arici, S. Dikbas, and Y. Altunbasak, "A histogram modification framework and its application for image contrast enhancement," *IEEE Trans. Image Process.*, vol. 18, no. 9, pp. 1921–1935, Sep. 2009.
[5] S. C. Huang, F. C. Cheng, and Y. S. Chiu, "Efficient contrast enhancement using adaptive gamma correction with weighting distribution," *IEEE Trans. Image Process.*, vol. 22, no. 3, pp. 1032–1041, Mar. 2013.
[6] T. Celik, "Two-dimensional histogram equalization and contrast enhancement," *Pattern Recog.*, vol. 45, no. 10, pp. 3810–3824, Oct. 2012.
[7] T. Celik and T. Tjahjadi, "Contextual and variational contrast enhancement," *IEEE Trans. Image Process.*, vol. 20, no. 12, pp. 3431–3441, Dec. 2011.
[8] T. Celik, "Spatial entropy-based global and local image contrast enhancement," *IEEE Trans. Image Process.*, vol. 23, no. 12, pp. 5298–5308, Dec. 2014.
[9] H. Demirel, G. Anbarjafari, and M. N. S. Jahromi, "Image equalization based on singular value decomposition," in *Proc. IEEE 23rd ISCIS*, 2008, pp. 1–5.
[10] E. Lee, S. Kim, W. Kang, D. Seo, and J. Paik, "Contrast enhancement using dominant brightness level analysis and adaptive intensity transformation for remote sensing images," *IEEE Geosci. Remote Sens. Lett.*, vol. 10, no. 1, pp. 62–66, Jan. 2013.
[11] J. H. Jang, S. D. Kim, and J. B. Ra, "Enhancement of optical remote sensing images by subband-decomposed multiscale retinex with hybrid intensity transfer function," *IEEE Geosci. Remote Sens. Lett.*, vol. 8, no. 5, pp. 983–987, Sep. 2011.
[12] G. Zhang, Q. Chen, and Q. Sun, "Illumination normalization among multiple remote-sensing images," *IEEE Geosci. Remote Sens. Lett.*, vol. 11, no. 9, pp. 1470–1474, Sep. 2014.
[13] C. E. Shannon, "A mathematical theory of communication," *Bell Syst. Tech. J.*, vol. 27, no. 3, pp. 379–423, Jul. 1948.
[14] J. Shin and R. H. Park, "Histogram-based locality-preserving contrast enhancement," *IEEE Signal Process. Lett.*, vol. 22, no. 9, pp. 1293–1296, Sep. 2015.
[15] A. Michelson, *Studies in Optics*. New York, NY, USA: Courier Corp., 1995.